

DARK MATTER SUBHALOS AND THE DWARF SATELLITES OF THE MILKY WAY

PIERO MADAU¹, JÜRGE DIEMAND^{1,2}, & MICHAEL KUHLEN³

(Accepted February 14, 2008)

ABSTRACT

The Via Lactea simulation of the cold dark matter halo of the Milky Way predicts the existence of many thousands of bound subhalos with masses above a few $\times 10^6 M_\odot$, distributed approximately with equal mass per decade of mass. Here we show that: a) a similar steeply rising subhalo mass function is also present at redshift $z = 0.5$ in an elliptical-sized halo simulated with comparable resolution in a different cosmology. Compared to Via Lactea, this run produces nearly a factor of two more subhalos with large circular velocities; b) the fraction of Via Lactea mass brought in by subhalos that have a surviving bound remnant today within r_{200} and with present-day peak circular velocity $V_{\max} > 2 \text{ km s}^{-1}$ ($> 10 \text{ km s}^{-1}$) is 45% (30%). Most of the Via Lactea mass is acquired in resolved discrete clumps, with no evidence for a significant smooth infall; c) because of tidal mass loss, the number of subhalos surviving today that reached a peak circular velocity of $> 10 \text{ km s}^{-1}$ throughout their lifetime exceeds half a thousand, five times larger than their present-day abundance and more than twenty times larger than the number of known satellites of the Milky Way; e) unless the circular velocity profiles of Galactic satellites peak at values significantly higher than expected from the stellar line-of-sight velocity dispersion, only about one in five subhalos with $V_{\max} > 20 \text{ km s}^{-1}$ today must be housing a luminous dwarf. Any mechanism that suppresses star formation in small subhalos must start acting early, at redshift $z > 3$; f) nearly 600 halos with masses greater than $10^7 M_\odot$ are found today in the “field” between r_{200} and $1.5r_{200}$, i.e. small dark matter clumps appear to be relatively inefficient at forming stars even well beyond the virial radius; g) the observed Milky Way satellites appear to follow the overall dark matter distribution of Via Lactea, while the largest simulated subhalos today are found preferentially at larger radii; h) subhalos have central densities that increase with V_{\max} and reach $\rho_{\text{DM}} = 0.1 - 0.3 M_\odot \text{ pc}^{-3}$, comparable to the central densities inferred in dwarf spheroidals with core radii $> 250 \text{ pc}$.

Subject headings: cosmology: theory – dark matter – galaxies: dwarfs – galaxies: formation – galaxies: halos – methods: numerical

1. INTRODUCTION

In the standard cosmological paradigm of structure formation (Λ CDM), the universe is dominated by cold, collisionless dark matter, and objects like the halo of our Milky Way are assembled via the hierarchical merging and accretion of smaller progenitors. Subunits collapse at high redshift, and when they merge into larger hosts their high densities allow them to resist the strong tidal forces that act to destroy them. Indeed, numerical simulations have shown that CDM halos are lumpy, teeming with self-bound subhalos on all resolved mass scales. It is now well established that the predicted subhalo counts vastly exceed the number of observed satellites of the Milky Way (Moore et al. 1999a; Klypin et al. 1999), a “missing satellite” or “substructure” problem that has been the subject of many recent studies. While some models have attempted to solve the apparent small-scale difficulties of CDM at a more fundamental level, i.e. by reducing small-scale power (e.g. Kamionkowski & Liddle 2000; Colín et al. 2000), astrophysical solutions that quench gas accretion and star formation in small halos have also been proposed as a plausible way out. The latter category includes cosmic reionization (e.g.

Bullock et al. 2000; Benson et al. 2002; Somerville 2002; Kravtsov et al. 2004; Moore et al. 2006), supernova feedback (e.g. Dekel & Silk 1986; Mac Low & Ferrara 1999; Mori et al. 2002), and gas stripping by ram pressure (e.g. Mayer et al. 2006) as favourite suppression mechanisms. Despite a wealth of ideas, however, a full characterization of the substructure problem is limited by three main uncertainties: 1) the old tally of Milky Way luminous satellites is very incomplete, and is being rapidly revised (e.g. Belokurov et al. 2007) by the discovery of a new, large population of ultra-faint dwarfs in the Sloan Digital Sky Survey (SDSS); 2) in cosmological N -body simulations, the ability of subhalos to survive the hierarchical clustering process as substructure within the host is particularly sensitive to resolution issues, as subhalos with numerically softened central densities are more easily disrupted by tidal forces (e.g. Moore et al. 1996; Diemand et al. 2007a); and 3) a detailed comparison between theory and observation in terms of, e.g., the peak circular velocity (V_{\max}) of subhalos is hampered by the fact that V_{\max} for the observed Milky Way satellites is poorly constrained by stellar velocity dispersion measurements (e.g. Strigari et al. 2007a).

“Via Lactea”, the highest-resolution simulation of galactic substructure to date (Diemand et al. 2007a,b; Kuhlen et al. 2007) offers the best opportunity for a systematic investigation of the missing satellite problem. Several of the newly discovered ultra-faint Milky Way satellites have estimated total masses just in excess of

Electronic address: diemand@ucolick.org, mqk@ias.edu, pmadau@ucolick.org

¹ Department of Astronomy & Astrophysics, University of California, Santa Cruz, CA 95064.

² Hubble Fellow.

³ Institute for Advanced Studies, Einstein Drive, Princeton, NJ 08540.

$10^6 M_\odot$ (like Leo IV, Coma Berenices, Canes Venatici II, see Simon & Geha 2007): such small dwarf galaxies are typically resolved in Via Lactea with > 50 dark matter particles, i.e. with a particle mass that is two dex smaller than in Moore et al. (1999b), three dex smaller than in Klypin et al. (1999), and more than one dex smaller than in the Diemand et al. (2004) and Gao et al. (2004) simulations of galaxy halos. Via Lactea follows the formation of a Milky Way-sized halo in a *WMAP* 3-year cosmology: within its r_{200} (the radius enclosing an average density 200 times the mean matter value), more than 2000 subhalos can be identified at $z = 0$ with $M_{\text{sub}} > 4 \times 10^6 M_\odot$, distributed approximately with equal mass per decade of mass. Of these, 40 are found within 50 kpc, a region that appeared practically smooth in previous simulations. Interestingly, the number of dwarf satellites in the inner halo of the Milky Way has recently tripled. Six dwarfs are currently known within 50 kpc of the Galactic Center: the LMC, Sagittarius, Ursa Major II, Coma Berenices, Willman 1, and Segue 1 (Mateo 1998; Willman et al. 2006; Zucker et al. 2006; Belokurov et al. 2007), for an estimated total number (after correcting for the SDSS sky coverage) of order 25. Note, however, that Willman 1 and Segue 1 lie at the uncertain boundary between dark matter-dominated dwarfs and globular clusters.

The apparent conflict between the Galaxy’s relatively smooth stellar halo and the extremely clumpy dark matter distribution of Via Lactea raises a number of important questions. First and foremost, is the amount of substructure found in Via Lactea typical of galaxy halos? If so, how efficiently does gas accretion, cooling, and star formation need to be suppressed as a function of subhalo mass to explain the observed abundance of dwarfs? Because of tidal mass loss, many of the subhalos that have small masses and circular velocities at the present epoch were considerably more massive and could have formed stars in the past. Does a single gas removal/star formation quenching mechanism determine the nature/fate of the subhalo population? What subset of subhalos has properties similar to the known stellar subsystems of the Milky Way? How does a dwarf’s luminosity relate to the mass evolutionary history of its host subhalo? Is the star formation suppression mechanism a strong function of the environment, or are small dark matter clumps inefficient at forming stars even beyond the virial radius of the Milky Way? We address some of these issues here. The paper is organized as follows. In §2 we compare the amount and distribution of Via Lactea substructure with that measured in an elliptical-sized halo simulated with comparable resolution in a different cosmology. In §3 we show that, because of late tidal mass loss, the number of subhalos that reached dwarf-galaxy sizes before accretion onto Via Lactea is much larger than their abundance today and the abundance of known Milky Way satellites. If substructure mass regulates star formation, then for a given mass threshold many more subhalos should have been able to build a sizeable stellar mass at some point in the past than indicated by their present-day abundance. Sections 4 and 5 discuss the main constraints on mechanisms for the suppression of star formation in small subhalos. The subhalo radial distribution and central dark matter densities are discussed and compared to the observations in §6. Finally, we present a brief summary

and our conclusions in §7.

2. CDM SUBSTRUCTURE IN GALAXY HALOS

The Via Lactea simulation was performed with the PKDGRAV tree-code (Stadel 2001) and employed multiple mass particle grid initial conditions generated with the GRAFICS2 package (Bertschinger 2001). The high resolution region was sampled with 234 million particles of mass $m_p = 2.1 \times 10^4 M_\odot$ and evolved with a force resolution of 90 pc starting from redshift 50. We adopted the best-fit cosmological parameters from the *WMAP* 3-year data release (Spergel et al. 2007): $\Omega_M = 0.238$, $\Omega_\Lambda = 0.762$, $H_0 = 73 \text{ km s}^{-1} \text{ Mpc}^{-1}$, $n = 0.951$, and $\sigma_8 = 0.74$. The $z = 0$ host halo mass within $r_{200} = 389$ kpc is $M_{\text{host}} = 1.77 \times 10^{12} M_\odot$. Its circular velocity profile reaches a peak of $V_{\text{host}} = 181 \text{ km s}^{-1}$ at $r_{V_{\text{host}}} = 62$ kpc. Note that the size of the Galaxy halo is still quite uncertain: since the effects of disk formation on the total mass distribution are still poorly constrained, the possible range of dark matter halo sizes that could form and host a 220 km s^{-1} disk is quite large, with V_{host} between 150 and 220 km s^{-1} (Klypin et al. 2002). When comparing Via Lactea to the Milky Way, this uncertainty allows one to rescale velocities and distances by $\pm 25\%$, and subhalo abundances above a given V_{max} by about a factor of $1.25^3 = 2$. A comparable uncertainty in the abundances comes from halo-to-halo scatter (e.g. Reed et al. 2005). Throughout this paper we will for simplicity assume that Via Lactea matches the properties of the Milky Way halo closely, but the substantial uncertainties mentioned above should always be kept in mind.

For comparison purposes, we have run another simulation, termed “1e8Ell”, that follows the formation of a more massive host halo with $M_{\text{host}} = 1.34 \times 10^{13} M_\odot$, $r_{200} = 512$ kpc, $V_{\text{host}} = 390 \text{ km s}^{-1}$ and $r_{V_{\text{host}}} = 116$ kpc. The high resolution region of this second run was sampled with 136,432,000 particles of mass $m_p = 1.8 \times 10^5 M_\odot$ and evolved from redshift 59.5 down to $z = 0.47$ with a force resolution of 162 pc. For 1e8Ell the best-fit cosmological parameters from the *WMAP* 1-year data release (Spergel et al. 2003) were adopted: $\Omega_M = 0.268$, $\Omega_\Lambda = 0.732$, $H_0 = 71 \text{ km s}^{-1} \text{ Mpc}^{-1}$, $n = 1$, and $\sigma_8 = 0.9$.

In both runs subhalos were identified using the phase-space friends-of-friends algorithm 6DFOF described in Diemand et al. (2006). Around the centers of all groups with at least 16 members, spherical density profiles were constructed, and the resulting circular velocity profiles were fitted with the sum of a Navarro, Frenk, & White (1997) profile and a constant density background. Subhalo tidal masses were assigned according to the definition given in Diemand et al. (2007a). The wealth of substructure resolved in our elliptical-sized halo is comparable to Via Lactea and is clearly seen in Figure 1. The halo finder algorithm identifies comparable numbers of dark matter clumps within the virial radius of Via Lactea at $z = 0$ and that of 1e8Ell at $z = 0.47$. Figure 2 shows the differential and cumulative subhalo mass functions within r_{200} for both runs. Substructure extends down to the smallest mass scales reliably resolved: as shown by Diemand et al. (2007a), numerical resolution effects start to flatten the mass distribution of subhalos below about 200 particles, and the maximum circular velocity distribution below $V_{\text{max}}/V_{\text{host}} \approx 0.02$.

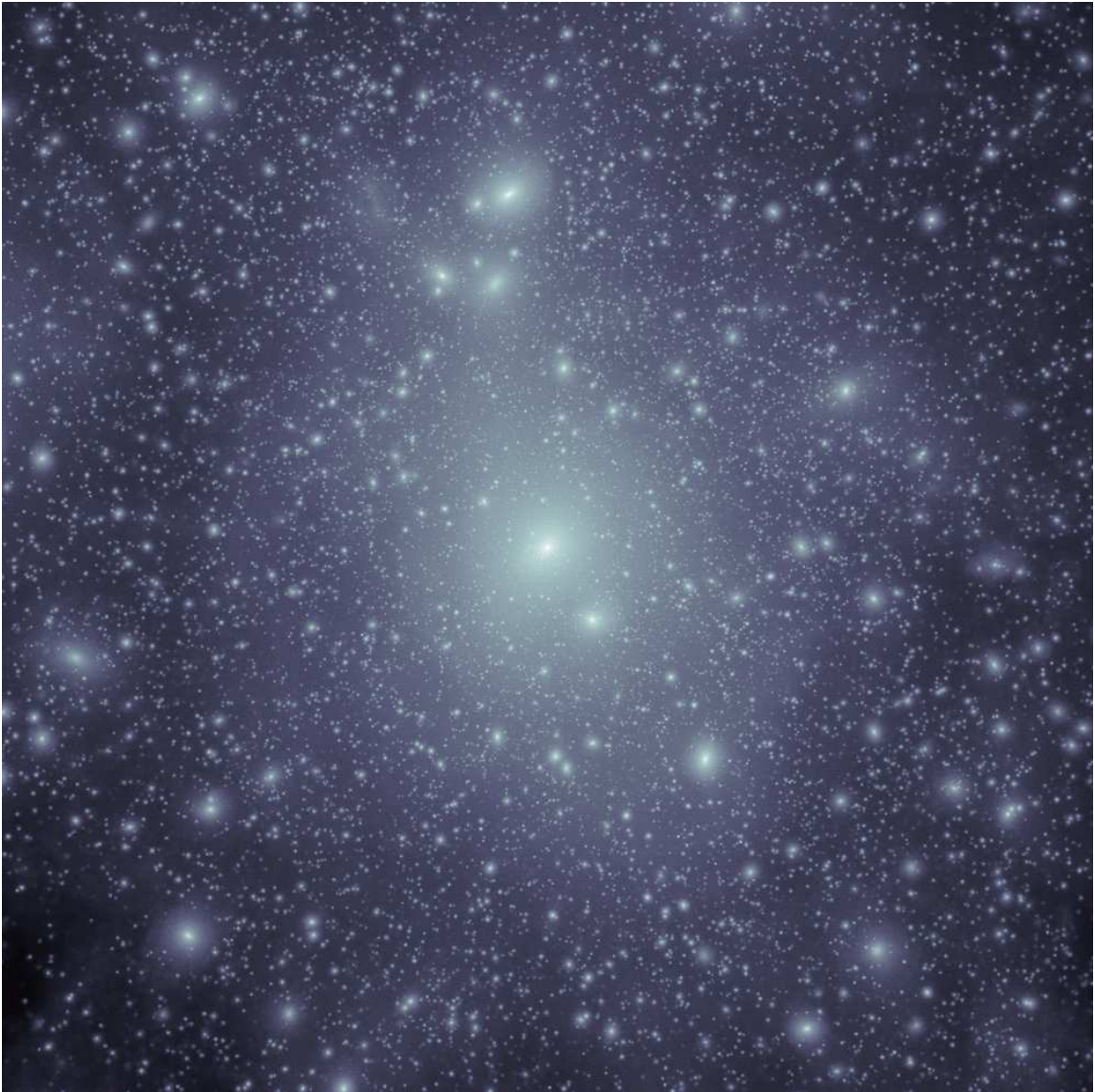


FIG. 1.— Projected dark matter density-square map of our simulated elliptical-sized halo (“1e8Ell”) at $z = 0.47$. The image covers an area of 980×980 physical kpc, and the projection goes through a 980 kpc-deep cuboid containing a total of 120 million particles and 25,000 identified subhalos. The logarithmic color scale covers 24 decades in density-square.

In the range $200m_p < M_{\text{sub}} < 0.01M_{\text{host}}$, the best-fit slope of the differential distribution, $dN/dM_{\text{sub}} \propto M_{\text{sub}}^\alpha$, is $\alpha = -1.86 \pm 0.02$ for 1e8Ell and $\alpha = -1.90 \pm 0.02$ for Via Lactea. In the same mass range the cumulative mass function has slope -0.92 for 1e8Ell and -0.97 for Via Lactea. Both simulations are therefore characterized by steeply rising subhalo counts that, in the case of Via Lactea, correspond to approximately equal mass per substructure mass decade: most subhalos are of low mass. Figure 3 (left panel) depicts the fraction of the host halo mass within a sphere of radius r_{200} that is bound up in substructure less massive than M_{sub} , $f_{\text{sub}}(< M_{\text{sub}})$ as a function of $M_{\text{sub}}/M_{\text{host}}$. We measure a total mass fraction in substructure that is about 5% in Via Lactea and exceeds 9% in 1e8Ell: its radial distribution can be approximated as $f_{\text{sub}}(< r) \propto r$ for $0.1 < r/r_{200} < 1$. Because of the steepness of the cumulative mass function, these fractions appear to be converging rather

slowly at the small-mass end: more than 1% of the host mass is found in clumps with $M_{\text{sub}}/M_{\text{host}} < 10^{-5}$. The amount of massive substructure is expected to increase with host halo mass since more massive hosts form later and dynamical friction and tidal-stripping have less time to operate (Gao et al. 2004; Zentner et al. 2005; van den Bosch et al. 2005). For the same reason, parent halos of a given mass will have a larger abundance of subhalos at higher redshifts than their present-day counterparts. However, when comparing $z = 0$ clusters with galaxy halos these effects are smaller than the observed halo-to-halo scatter in subhalo abundance (Diemand et al. 2004; Reed et al. 2005). Variation in the slope and normalization of the power spectrum can also affect the amount of subhalos significantly, especially their circular velocity function (Zentner & Bullock 2003).

It is conventional to discuss the substructure popula-

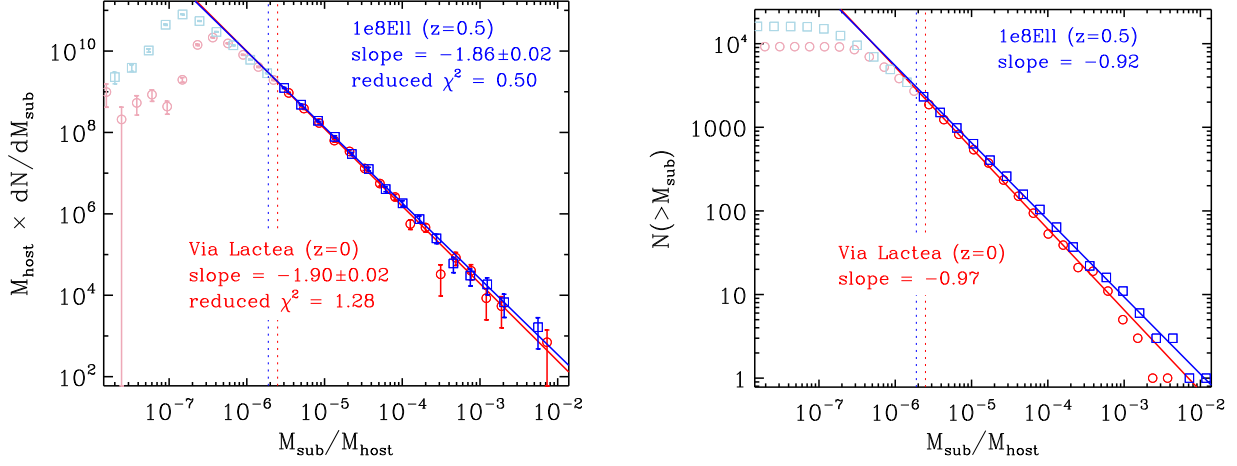


FIG. 2.— Differential (left panel) and cumulative (right panel) subhalo mass functions within r_{200} for 1e8Ell at $z = 0.47$ (blue square points) and Via Lactea at $z = 0$ (red square points), together with power-law fits (solid lines) in the range $200m_p < M_{\text{sub}} < 0.01M_{\text{host}}$.

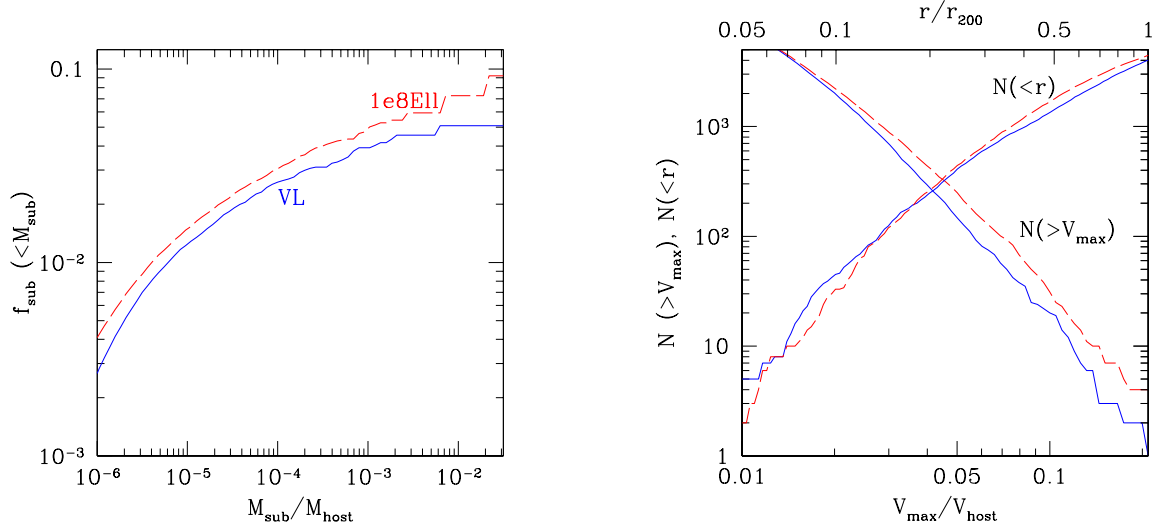


FIG. 3.— Left panel: Fraction of the host halo mass that is bound up in substructure less massive than M_{sub} as a function of $M_{\text{sub}}/M_{\text{host}}$. Lower solid curve: Via Lactea. Upper dashed curve: 1e8Ell. Right panel: Cumulative maximum circular velocity function, $N(>V_{\text{max}})$, for all subhalos within r_{200} , as a function of $V_{\text{max}}/V_{\text{host}}$. There are 7932 subhalos with $V_{\text{max}}/V_{\text{host}} > 0.01$ in Via Lactea, versus 8005 in 1e8Ell. Also plotted is the radial distribution, $N(<r)$, of all mass-selected subhalos with $M_{\text{sub}}/M_{\text{host}} > 10^{-6}$ versus r/r_{200} . Solid curves: Via Lactea, $N(<r_{200}) = 4021$. Dashed curves: 1e8Ell, $N(<r_{200}) = 4447$.

tion of galaxy halos in terms of the circular velocity function. Figure 3 (right panel) shows the cumulative maximum circular velocity ($V_{\text{max}} \equiv \max\{\sqrt{GM_{\text{sub}}(<r)}/r\}$) functions for the entire subhalo population within the two hosts. These are well-fit by a power-law of the form

$$N(>V_{\text{max}}) = 100 V_{\text{max},10}^{-3} \quad (0.4 < V_{\text{max},10} < 3.5) \quad (1)$$

for Via Lactea, and

$$N(>V_{\text{max}}) = 1500 V_{\text{max},10}^{-2.8} \quad (0.8 < V_{\text{max},10} < 5.5) \quad (2)$$

for 1e8Ell, with fractional errors not exceeding 20% in both cases. (Here $V_{\text{max},10} \equiv V_{\text{max}}/10 \text{ km s}^{-1}$.) When V_{max} is normalized to the maximum circular velocity of the host, V_{host} , the two substructure velocity functions are very similar at the low end, and become more discrepant at larger V_{max} values. There are 110 sub-

halos above $V_{\text{max}} = 10 \text{ km s}^{-1} = 0.056 V_{\text{host}}$ in Via Lactea, compared to 170 above $V_{\text{max}} = 22.5 \text{ km s}^{-1} = 0.056 V_{\text{host}}$ in 1e8Ell. As already discussed above, it is well known that large subhalos (roughly within a factor of 30 of the maximum circular velocity of the host) constitute a transient population that continuously declines from mass-loss effects. The Via Lactea run has now shown that small-scale substructure is instead more persistent and independent of the age and size of the host (Diemand et al. 2007b), consistent with predictions from semi-analytic models (Zentner et al. 2005). This is also supported by the left panel of Figure 3: within the range $10^{-6} \lesssim M_{\text{sub}}/M_{\text{host}} \lesssim 10^{-2}$, the measured substructure mass fractions $f_{\text{sub}}(<M_{\text{sub}})$ in the two simulations differ by less than $\sim 40\%$. While the similarity between the two objects is noteworthy, we caution that such close agreement could be just a coincidence, and substantial amount

of halo-to-halo scatter may be present in the abundance of small-scale substructure.⁴ The larger clumpiness of 1e8Ell is dominated by its three surviving subhalos with $M_{\text{sub}}/M_{\text{host}} > 0.006$, versus none this massive identified in Via Lactea.

The right panel of Figure 3 also shows the radial distribution of subhalos as a function of r/r_{200} . In the range $0.1 < x \equiv r/r_{200} < 1$, the abundance profiles of *mass-selected* subhalos are very similar and well fit by

$$N(< x) = N(< r_{200}) \frac{12x^3}{1 + 11x^2}. \quad (3)$$

This distribution agrees well with those presented by Diemand et al. (2004) and Gao et al. (2004), extending the validity of these previous results down to $M_{\text{sub}} > 10^{-6} M_{\text{host}}$. Subhalos do not trace the matter distribution of the host: tidal disruption is most effective in the inner halo, which leads to an antibias in the abundance profile of substructure relative to the smooth background, i.e. the radial distribution of subhalos above a given mass is much flatter than that of the dark matter in the host halo. This antibias is less pronounced if subhalos are selected by today's peak circular velocity instead. The threshold $V_{\text{max}}/V_{\text{host}} > 0.02$ yields a sample of 2016 and 2334 subhalos in Via Lactea and 1e8Ell, respectively. In the range $0.01 < x < 1$, the abundance profiles of these V_{max} -selected subhalos is well fit by

$$N(< x) = N(< r_{200}) \frac{20x^{2.9}}{1 + 19x^{1.9}}. \quad (4)$$

3. FOSSIL RECORDS AND MISSING SATELLITES

The Via Lactea and 1e8Ell runs discussed above show that, in the standard CDM paradigm, galaxy halos are filled with tens of thousands low-mass subhalos, about an order of magnitude more than found in previous simulations. Subhalos lose mass from the outside in through tidal stripping, the largest average mass fraction being lost at the first pericenter passage (Diemand et al. 2007b). Larger clumps retain less of their mass as they sink quickly towards the host center due to dynamical friction, while the retained mass fraction is larger for initially lighter subhalos that are less affected by dynamical friction and stay in place. As many as 97% of all well-resolved [$> 5,000$ particles, $V_{\text{max}}(z) > 10 \text{ km s}^{-1}$] subhalos identified in Via Lactea at $z = 1$ do not lose their identity and have a surviving $z = 0$ remnant. This can be compared with the 47% that survive from $z = 4$ and the 20% from $z = 10$. Note that not all the subunits without a remnant today are totally disrupted to become part of the “smooth” host halo, some simply merge into larger substructure that eventually survives down to the present epoch.

It is interesting to know, at the high-resolution limit of our simulations, what fraction of the Via Lactea's host halo mass was accreted in identifiable clumps, and compare it with the mass brought in by subhalos that have a surviving bound remnant within r_{200} at the present epoch. The latter is expected to be significantly smaller

than the former, since many major mergers at early times leave no surviving $z = 0$ subhalos. We have therefore traced backward in time the progenitors of present-day remnants in each simulation snapshot, measured the *maximum mass* they had at any point during their history i.e. before they suffered tidal mass losses, summed up this mass over all subhalos within r_{200} having peak circular velocity $> V_{\text{max}}$, and divided the result by the mass of Via Lactea today. The total mass fraction, $f_{\text{acc}}(> V_{\text{max}})$, brought in by surviving substructure is plotted in Figure 4 as a function of V_{max} , and is found to exceed 45% for $V_{\text{max}} > 2 \text{ km s}^{-1}$. There are (14, 109, 873) subhalos today with $V_{\text{max}} > (20, 10, 5) \text{ km s}^{-1}$, which contributed (19, 30, 39)% of the mass of Via Lactea. Only 9-10% of the total material they brought in remains in self-bound identifiable clumps at the present-epoch, the rest having been removed by tidal effects to become part of the “smooth” halo component. Note that numerical effects lead to less cuspy subhalos that suffer from artificially high-mass loss, especially in the inner halo where tidal forces are strong (Kazantzidis et al. 2004). Figure 4 also shows the total mass accreted in clumps, $f_{\text{acc}}(> V_{\text{max,p}})$, independently of whether these survive or not to the present day. This is plotted against the highest V_{max} reached by subunits throughout their lifetime, a quantity we refer to as ‘ $V_{\text{max,p}}$ ’ (see also Kuhlen et al. 2007). Interestingly, more than 97% of the Via Lactea mass is acquired in resolved discrete clumps with no evidence for significant smooth accretion.

The large tidal mass losses suffered by massive subhalos have obvious implications for astrophysical solutions to the satellite problem. The leading scenario for reconciling the mismatch between luminous and dark substructure in the Milky Way posits that stars are able to form continuously and efficiently only in halos above a certain mass threshold, a threshold determined by the inability of shallow potential wells to accrete intergalactic gas photoionized by the ultraviolet (UV) background and/or to retain gas blown out by supernova explosions. There are slightly in excess of 20 dwarf galaxies known to orbit the Milky Way. After correcting for the sky coverage of the fifth data release of the SDSS, i.e. after weighing each of the new ultra-faint dwarfs by a factor ~ 6 , the total number of satellites is probably around 60-70 (Simon & Geha 2007; Koposov et al. 2007) down to a surface brightness limit of $\mu_V = 30 \text{ mag arcsec}^{-2}$. A solution to the substructure problem suggested by Stoehr et al. (2002) and Hayashi et al. (2003) would be to place the luminous dwarfs in the most massive subhalos *at the present epoch*, suitably adjusting the mass (or peak circular velocity) threshold for efficient galaxy formation. There are 65 subhalos today in Via Lactea (within r_{200}) with $M_{\text{sub}} > 1.4 \times 10^8 M_{\odot}$ or $V_{\text{max}} > 12 \text{ km s}^{-1}$: the paucity of Milky Way satellites would then be simply explained by the inhibition of star formation below the above values of M_{sub} and V_{max} . Baryonic material falling in the dark matter potential well will be shock heated to the effective virial temperature of the host, compressed, and eventually cool and fragment into stars. A circular velocity threshold of 12 km s^{-1} corresponds to a virial temperature

$$T_{\text{vir}} = \frac{\mu m_p V_{\text{max}}^2}{2k_B} < 8700 \mu \text{ K}, \quad (5)$$

⁴ Note that the measured abundance of small-scale substructure may also be sensitive to our change from a *WMAP* year-1 (1e8Ell) to year-3 (Via Lactea) cosmology, especially to the lower normalization of the power-spectrum σ_8 .

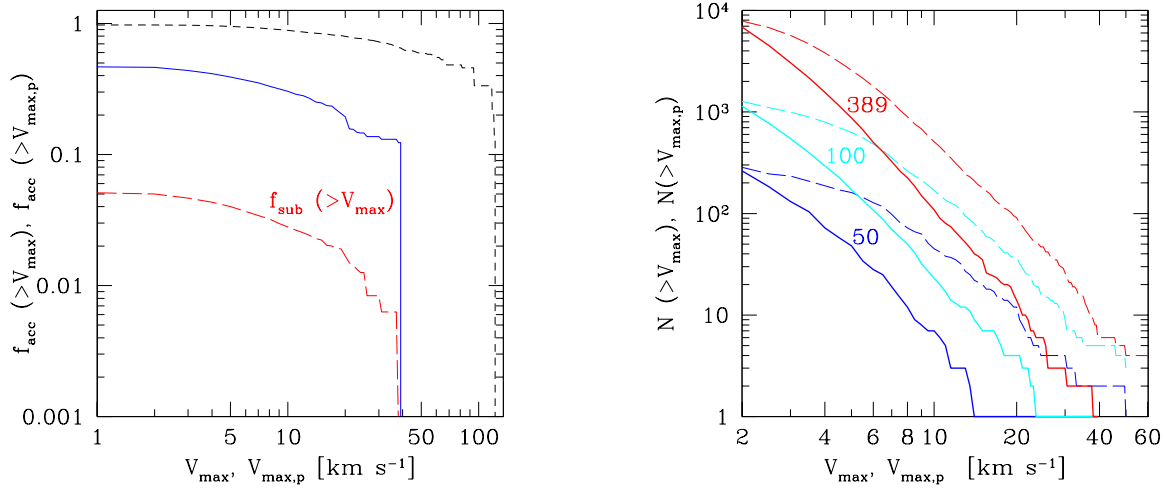


FIG. 4.— *Left panel:* Via Lactea accreted mass fraction $f_{\text{acc}}(>V_{\text{max}})$ (total mass brought in by all substructure *surviving today* within r_{200} above V_{max} , normalized to the mass of the host), as a function of today’s subhalo circular velocity (*upper solid curve*). For comparison, we also plot the mass $f_{\text{acc}}(>V_{\text{max,p}})$ brought in by all resolved subunits as a function of the highest maximum circular velocity reached throughout their lifetime, $V_{\text{max,p}}$ (*upper short-dashed curve*). The long-dashed lower curve shows the mass fraction $f_{\text{sub}}(>V_{\text{max}})$ that remains in self-bound identifiable clumps at the present-epoch. *Right panel:* Cumulative circular maximum velocity function of all subhalos today within 50, 100, and 389 kpc (*solid lines, from bottom to top*). *Dashed lines:* Same for a sample of subhalos having a surviving bound remnant today and selected by their $V_{\text{max,p}}$.

where μ is the mean molecular weight. Figure 5 shows the cumulative number of Via Lactea subhalos as well as all Milky Way satellite galaxies within 420 kpc (the distance of Leo T, Irwin et al. 2007) as a function of circular velocity. The current available data are summarized in Table 1. The data points in the figure include all the previously known dwarfs (Mateo 1998) plus the new circular velocity estimates of the ultra-faint Milky Way satellites from Simon & Geha (2007), plus Boötes (Munoz et al. 2006) and Willman 1 (Martin et al. 2007). They have been plotted assuming a maximum circular velocity of $V_{\text{max}} = \sqrt{3}\sigma$ (Klypin et al. 1999), where σ is the measured stellar line-of-sight velocity dispersion, i.e. assuming a stellar spherical density profile $\propto r^{-3}$ in a singular isothermal potential. Note that the assumption of a constant multiplicative factor between V_{max} and σ is merely the simplest thing to do, and is not likely to hold on a case-by-case basis. Detailed modeling of the radial velocity dispersion profile, allowing for variations in the DM mass distribution and the stellar velocity anisotropy (Strigari et al. 2007a), would be preferable, but is currently only available for a subset of all known dwarfs.

If the stellar systems deeply embedded in dwarf spheroidals remain largely unaffected by tidal stripping (this is clearly not the case, e.g., for Ursa Major II and Sagittarius), then the mass removal of large fractions of their original halo mass by tidal effects may make solutions in which luminosity tracks *current* subhalo mass somewhat misleading. Our simulations show and quantify better than before that many of the dark matter clumps that have small masses and circular velocities at the present epoch were considerably more massive and should have formed stars in the past (e.g. Kravtsov et al. 2004). We illustrate this point in Figure 4 (right panel), which shows the cumulative circular maximum velocity function of substructure within 50, 100, and 389 kpc.

Also plotted, for comparison, is the abundance of *surviving* subhalos selected instead by the highest circular velocity they reached throughout their lifetime, $V_{\text{max,p}}$. Subhalos will reach their $V_{\text{max,p}}$ at a redshift z_{max} before falling into Via Lactea: this type of circular velocity selection is designed then to remove the bias introduced by tidal mass losses, and to *highlight the subhalos that may have started shining before being accreted by their host*. Within r_{200} , the number of massive galactic subhalos that reached a peak circular velocity in excess of 10 km s^{-1} at some point during their history is 510, about *five times larger* than their present-day abundance. This ratio increases with increasing $V_{\text{max,p}}$ and decreasing radius: a) above a virial temperature $T_{\text{vir}} = 10,000 \text{ K}$, or a circular velocity $V_{\text{max}} = 16.7 \text{ km s}^{-1}$ ($\mu = 0.59$ for fully ionized primordial gas), gas can cool efficiently and fragment via excitation of hydrogen Ly α . The number of subhalos within r_{200} that reached this “atomic cooling” mass at some point in the past is 135, nearly *six times larger* than their present-day abundance; b) within the inner 50 kpc there is today only one subhalo with $V_{\text{max}} > 16.7 \text{ km s}^{-1}$, but there are 16 surviving remnants that had this peak circular velocity and were more massive at earlier times. *If substructure mass regulates star formation, then for a given mass threshold many more subhalos should have been able to build a sizeable stellar mass at some point in the past than indicated by their present-day abundance.*

It is important then to investigate the consequences of a mass (or circular velocity) cut that picked instead the top (say) 65 most massive (or largest $V_{\text{max,p}}$) subhalos at all epochs as the hosts of the known Milky Way dwarfs. Following Diemand et al. (2007b), such or similar samples have been termed “LBA” (for “largest before accretion” subhalos) by Strigari et al. (2007a) and Simon & Geha (2007). The idea behind this selection

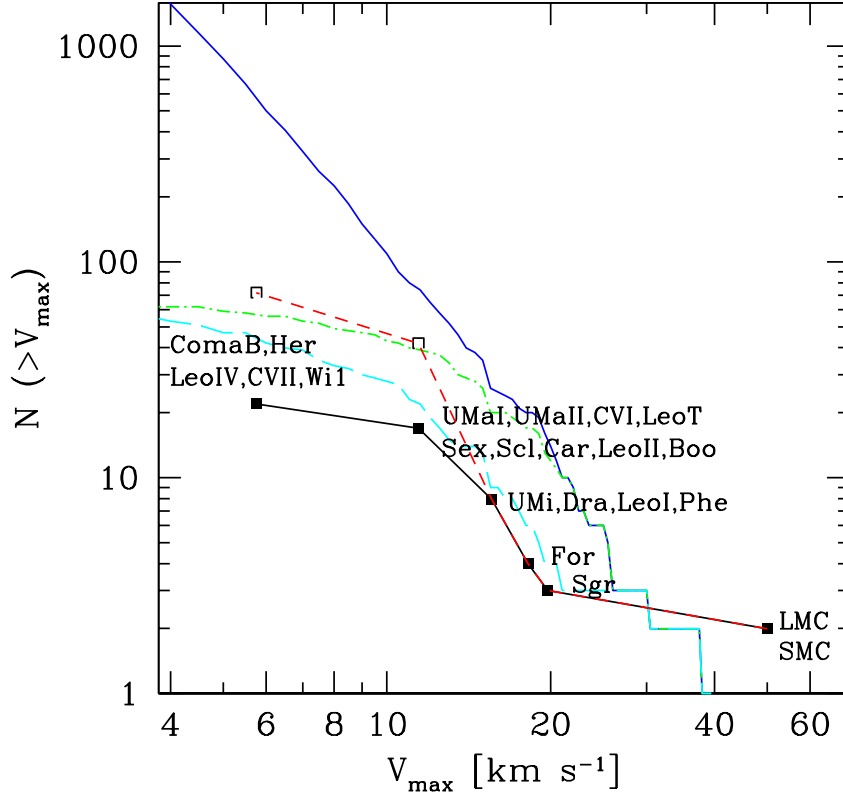


FIG. 5.— Cumulative number of Via Lactea subhalos within r_{200} (solid curve) as well as all Milky Way satellite galaxies within 420 kpc (filled squares), as a function of circular velocity. The data points are from Mateo (1998), Simon & Geha (2007), Munoz et al. (2006), and Martin et al. (2007), and assume a maximum circular velocity of $V_{\max} = \sqrt{3}\sigma$ (Klypin et al. 1999). The short-dashed curve connecting the empty squares shows the expected abundance of luminous satellites after correcting for the sky coverage of the SDSS. Dash-dotted curve: circular velocity distribution for the 65 largest $V_{\max,p}$ subhalos before accretion (LBA sample). Long-dashed curve: circular velocity distribution for the “fossil of reionization” EF sample. This includes the 61 largest (sub)halos at $z = 13.6$ [$V_{\max}(z = 13.6) > 4 \text{ km s}^{-1}$] plus the 4 (sub)halos that reach a $V_{\max,p} > 38 \text{ km s}^{-1}$ after the epoch of reionization and are not in the largest 61 at $z = 13.6$.

is to allow star formation only above a relatively large constant critical size, a scenario of permanently inefficient galaxy formation in all smallest systems, independently of time-varying changes in the environment like those triggered, e.g., by reionization. Today’s circular velocity distribution of our LBA sample is shown in Figure 5: interestingly, this sample includes 12 of the 14 subhalos above $V_{\max} = 20 \text{ km s}^{-1}$ identified today, and 26 of the 35 identified above $V_{\max} = 15 \text{ km s}^{-1}$, i.e. the most massive today and LBA subpopulations basically coincide at large values of V_{\max} .⁵ Therefore a solution to the substructure problem in which only the largest 50–100 $V_{\max,p}$ subhalos at all epochs were able to form stars efficiently would automatically place the luminous Milky Ways dwarfs in the most massive subhalos at the present epoch. To match the circular velocity function of the LBA sample, however, the observed dwarf spheroidals

(dSphs) must have circular velocity profiles that peak at values well in excess of the stellar velocity dispersion (see Fig. 5 and discussion below). Note that the cut in $V_{\max,p}$ instead of V_{\max} of the LBA sample requires star formation to be inhibited in all subhalos with $V_{\max,p} < 21.9 \text{ km s}^{-1}$ or virial temperature

$$T_{\text{vir}} = \frac{\mu m_p V_{\max,p}^2}{2k_B} < 17,000 \text{ K.} \quad (6)$$

4. SUPPRESSING DWARF GALAXY FORMATION

The two thresholds for efficient star formation given in equations (5) and (6) provide the correct total number of luminous Milky Way satellites (assumed to be around 60–70), not a match to the observed circular velocity function. A careful look at Figure 5 suggests two possible solutions to the mismatch problem:

1. stars in the Milky Way dSphs are deeply embedded within their dark matter halos. The halo circular velocity profiles peak well beyond the luminous radius at speeds significantly higher than expected

⁵ Note that the same is not true for the top 10 LBA subhalos (Kravtsov et al. 2004; Diemand et al. 2007b; Strigari et al. 2007a), as the largest $V_{\max,p}$ systems suffer the largest mass loss and are removed from the top ten list of more massive systems at $z = 0$.

TABLE 1
THE MILKY WAY SATELLITES

Name	Heliocentric distance (kpc)	σ (km s ⁻¹)	ρ_0 (M _⊙ pc ⁻³)	Core radius r_c (pc)	References
Segue 1	23	—	—	19	(1)
Sagittarius	24	11.4	0.07	550	(2)
Ursa Major II	32	6.7	1.14	81	(3),(4)
Willman 1	38	4.3	18	13	(5),(6)
Coma Berenices	44	4.6	2.1	41	(1),(3)
LMC	49	20.2	—	—	(2),(7)
SMC	58	27.5	—	—	(2),(8)
Boötes	60	6.6	0.34	145	(9),(10)
Boötes II	60	—	—	46	(11)
Ursa Minor	66	9.3	0.36	200	(2)
Sculptor	79	6.6	0.60	110	(2)
Draco	82	9.5	0.46	180	(2)
Sextans	86	6.6	0.06	335	(2)
Carina	101	6.8	0.17	210	(2)
Ursa Major I	106	7.6	0.25	197	(3)
Fornax	138	10.5	0.09	460	(2)
Hercules	138	5.1	0.10	205	(1),(3)
Canes Venatici II	151	4.6	0.49	85	(1),(3)
Leo IV	158	3.3	0.19	97	(1),(3)
Canes Venatici I	224	7.6	0.08	355	(3)
Leo II	233	6.7	0.24	178	(2),(12),(15)
Leo I	255	9.2	0.23	245	(13),(16)
Leo T	417	7.5	0.79	109	(3),(17)
Phoenix	420	8.9	0.14	310	(2),(14)

REFERENCES. — (1) Belokurov et al. 2007; (2) Mateo 1998; (3) Simon & Geha 2007; (4) Zucker et al. 2006; (5) Willman et al. 2006; (6) Martin et al. 2007; (7) van der Marel et al. 2002; (8) Harris & Zaritsky 2006; (9) Belokurov et al. 2006; (10) Munoz et al. 2006; (11) Walsh et al. 2007; (12) Bellazzini et al. 2005; (13) Mateo et al. 2007; (14) Young et al. 2007; (15) Coleman et al. 2007; (16) Bellazzini et al. 2005; (17) Irwin et al. 2007.

from the stellar line-of-sight velocity dispersion, i.e. $V_{\max} \sim 3\sigma$ as suggested by Stoehr et al. (2002) and Peñarrubia et al. (2007). This scenario would shift the data points in Figure 5 by about a factor $\sqrt{3}$ further to the right, making the mass distribution of the luminous Milky Way dwarf spheroidals agree with the steep mass function of the most massive Via Lactea subhalos today. Its main drawback is that it boosts the number of massive *inner* satellites to values that are difficult to reconcile with Λ CDM halos. There are five Milky Way dwarfs within 50 kpc of the Galactic Center with measured stellar velocity dispersions σ above 4 km s⁻¹: the SDSS ultra-faint Coma Berenices, Willman 1, and Ursa Major II, together with the LMC and Sagittarius. Correcting for the sky coverage of the SDSS and using the conversion $V_{\max} \sim 3\sigma$ would bring the total number of inner satellites above $V_{\max} \sim 12$ km s⁻¹ to twenty or so. By contrast, there are only three subhalos in Via Lactea with $d < 50$ kpc and $V_{\max} > 12$ km s⁻¹ today (see the right panel of Fig. 4). Note that, even at the resolution of Via Lactea, subhalos within (say) 50 kpc from the center may still be subject to numerical overmerging. We will compare in detail the radial distribution of Milky Way’s satellites and Via Lactea subhalos in the next section.

2. if $V_{\max} \sim \sqrt{3}\sigma$ instead, then the discrepancy between the number of *massive* substructure expected in Λ CDM and the known companions of the Milky Way can be solved if only approximately one out of five subhalos with $V_{\max} > 20$ km s⁻¹ today houses

a luminous dwarf satellite. Because of dynamical friction and tidal mass losses, the large subhalos that are today devoid of stars were typically more massive in the past. This scenario therefore requires star formation to be quenched in objects that reached peak circular velocities as large as 35 – 40 km s⁻¹ in the past.

To shed further light on the star formation suppression mechanism that is acting on galactic substructure we have plotted in Figure 6 (left panel) all Via Lactea subhalos that reached a $V_{\max,p} > 10$ km s⁻¹ at redshift z_{\max} . Out of a total of 510 subhalos, 318 reached their $V_{\max,p}$ at redshift $z_{\max} > 2$, 180 at $z_{\max} > 3$, and 80 at $z > 4$. The color coding indicates the different intervals of V_{\max} where those subhalos end up today. Clumps that were accreted earlier ($z_{\max} > 3$) are more heavily affected by tidal stripping and their $V_{\max,p}$ ’s drop by more than 67%. If stars can form continuously and efficiently only above a mass or circular velocity threshold, then clearly *any quenching mechanism must already be in place at early times*.

At a distance of 420 kpc and with a surface brightness of $\mu_V = 26.9$ mag arcsec⁻², Leo T has well-measured kinematics from both the stars and the gas, a stellar velocity dispersion of 7.5 ± 1.6 km s⁻¹, an estimated mass just short of 10^7 M_⊙, an absolute magnitude $M_V = -7.1$, and a total mass-to-light ratio (M/L_V) of 138 ± 71 (Irwin et al. 2007; Simon & Geha 2007; Ryan-Weber et al. 2007). The detection efficiency for satellites this luminous over the SDSS survey area is nearly unity, so only a handful of similar objects is expected over the whole sky. Even at distances well in

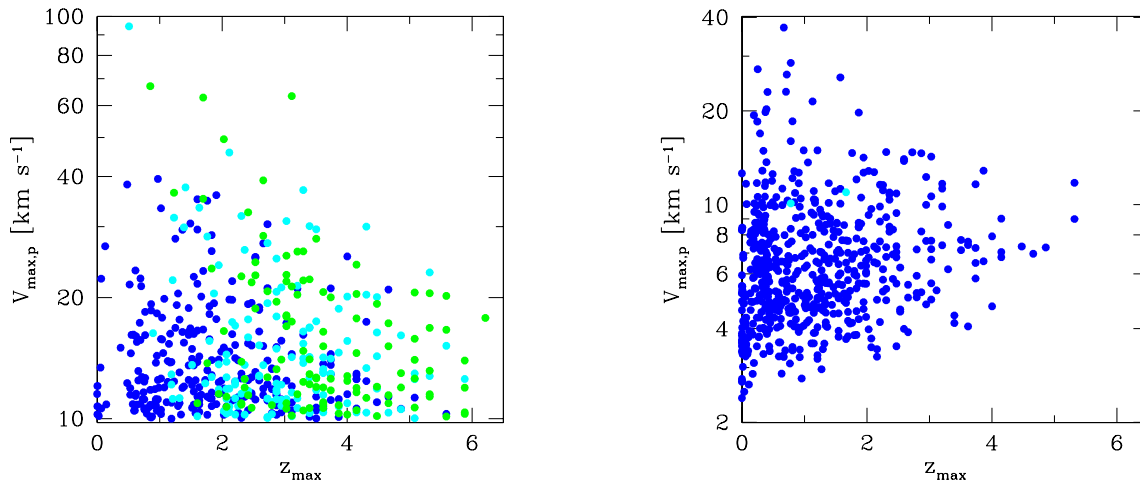


FIG. 6.— *Left panel:* All (510) Via Lactea subhalos that reached a $V_{\max,p} > 10 \text{ km s}^{-1}$ at redshift z_{\max} , plotted in the $V_{\max,p} - z_{\max}$ plane. The color coding indicates the different intervals of V_{\max} where those subhalos end up today: $V_{\max} > V_{\max,p}/2$ (blue dots), $V_{\max,p}/3 < V_{\max} < V_{\max,p}/2$ (cyan dots), $V_{\max} < V_{\max,p}/3$ (green dots). Clumps that were accreted earlier ($z_{\max} > 3$) are more heavily affected by tidal stripping and their $V_{\max,p}$'s drop by more than 67%. *Right panel:* Same (but on a different $V_{\max,p}$ scale) for the sample of 575 halos that lie today in the “field” between 389 kpc (r_{200}) and 584 kpc ($1.5r_{200}$) and are more massive than $10^7 M_{\odot}$. Most of these are accreted late ($z_{\max} \lesssim 1$) and suffer only moderate mass loss.

excess of 500 kpc, objects brighter than $M_V = -8$ would have been found by the SDSS (Koposov et al. 2007). In the right panel of Figure 6 we have plotted in the same $V_{\max,p} - z_{\max}$ plane (but on a different $V_{\max,p}$ scale) the sample of 575 halos that lie today in the “field” between 389 kpc (r_{200}) and 584 kpc ($1.5r_{200}$) and are more massive than $10^7 M_{\odot}$. And while this numerous subpopulation may be shining just under the detection threshold as ultra-faint dwarfs, it seems fair to conclude that *small dark matter clumps must be relatively inefficient at forming stars even well beyond the virial radius*. The figure shows that most of these “field” halos are newcomers, i.e. they are accreted late ($z_{\max} \lesssim 1$) and suffer only moderate mass loss. Contrary to what is invoked for more massive dwarf spheroidals sinking within 50-100 kpc from the Galactic Center (Mayer et al. 2007), gas stripping by ram pressure in a hot low-density Galactic corona is unlikely to be responsible for the truncation of star formation in this subpopulation. Indeed, while many of these field halos are former subhalos, i.e. passed through the host at some earlier time, only 15% of them had pericenters within 50 kpc.

5. A TOY MODEL OF REIONIZATION SUPPRESSION

A popular model for the suppression of gas accretion and star formation in small halos is the “reionization scenario”. In this hypothesis the observed dSphs correspond to the surviving substructure population that accreted a significant amount of gas before the epoch of reionization at redshift > 10 and achieved a potential well deep enough to form stars: after reionization, UV photoionization feedback results in the quenching of star formation in all newly forming subhalos below some mass threshold. While this general model has been investigated by a number of authors in the recent literature (e.g. Bullock et al. 2000; Benson et al. 2002; Somerville 2002; Kravtsov et al. 2004; Ricotti & Gnedin 2005;

Moore et al. 2006; Diemand et al. 2007a; Strigari et al. 2007a; Simon & Geha 2007), there are considerable differences in the specifics of its many variants.

The *Wilkinson Microwave Anisotropy Probe* (WMAP) 3-year data require the universe to be fully reionized by redshift $z = 11 \pm 2.5$ (Spergel et al. 2006). The reionization history of a given galaxy-forming region appears to depend strongly on the mass of its present-day halo, with higher mass systems forming earlier on average and thus being reionized earlier (Weinmann et al. 2007). Following Moore et al. (2006), let us assume that the region around the Milky Way was reionized around $z = 12 - 13$, i.e. when reionization was well advanced in the universe as a whole. Cosmological hydrodynamic simulations of early structure formation in a Λ CDM universe have found that a typical H_2 fraction in excess of 200 times the primordial value is produced after the collapse of halos with virial temperatures above 1000 K. This is large enough to efficiently cool the gas and allow it to collapse and form stars within a Hubble time unless significant heating occurs during this phase (e.g. Machacek et al. 2001; Yoshida et al. 2003; Kuhlen & Madau 2005). A virial temperature of 1200 K corresponds to a circular velocity of $V_{\max} = 4 \text{ km s}^{-1}$. Prior to reionization, at a redshift of 13.6, there are 61 halos with $V_{\max}(z = 13.6) > 4 \text{ km s}^{-1}$ in the Via Lactea simulation that will have a surviving bound remnant today within r_{200} . At this early epoch their masses range between $1.5 \times 10^6 M_{\odot}$ and $1.6 \times 10^8 M_{\odot}$, and only one object in the sample is above the critical mass threshold for atomic cooling. Let us assume that the observed dSphs are fossils of this first generation of small-mass galaxies, a hypothesis consistent with the fact that old populations with ages > 10 Gyr are the dominant stellar component of Milky Way dSphs (see e.g. Grebel 2000; Dolphin et al. 2005). A cosmic UV background at $z > 10$ has been shown to have little impacts on dwarf

galaxy-sized objects with $V_{\max} \gtrsim 10 \text{ km s}^{-1}$ that have already grown to a substantial overdensity when the ionizing radiation turns on and can self-shield against it (Dijkstra et al. 2004). The most massive of these early-forming objects (EF sample) may then retain a fraction of their gas even after reionization, and may undergo a later episode of star formation triggered e.g. by tidal shocking during their accretion into the parent halo. By contrast, after reionization breakthrough, photoionization heating leads to a dramatic increase in the temperature of the intergalactic medium, and gas cannot accrete and cool to fuel star formation in newly forming dark matter halos that are not sufficiently massive. The exact value of this threshold has been the subject of many studies, and depends on the redshift of collapse, the amplitude and spectrum of the ionizing background, and the ability of the system to self-shield against UV radiation (e.g. Efstathiou 1992; Thoul & Weinberg 1996; Navarro & Steinmetz 1997; Dijkstra et al. 2004). Here we assume that after reionization gas infall and cooling occurs only onto dwarf galaxy-sized objects that reach the threshold $V_{\max, \text{p}} > 38 \text{ km s}^{-1}$. This brings our EF sample to a total of 65 surviving subhalos (as in the LBA sample). Their present-day circular velocity function is shown in Figure 5, and it appears to reproduce reasonably well the velocity distribution of the known Milky Way satellites.

6. SUBHALO RADIAL DISTRIBUTION AND CENTRAL DENSITIES

The spatial distribution of luminous satellites provides another challenge to Λ CDM substructure models. Figure 7 compares the normalized cumulative radial distributions of the known Milky Way dwarfs to that of the oldest (EF) and highest $V_{\max, \text{p}}$ (LBA) dark matter subhalos of Via Lactea. For plotting and comparison purposes, we have placed Leo T and Phoenix within r_{200} . The observed satellites are clearly more biased to lie at small radii than both the LBA and the EF samples. The median distance of the observed satellites is 90 kpc, and the satellite distribution becomes even more compact after correcting for the SDSS sky coverage (see Fig. 7). This must be compared to a median distance of 110 kpc for the LBA and EF samples, and to 235 kpc for all Via Lactea subhalos. About 40% (50% after SDSS correction) of all Milky Way dwarfs are found within 60 kpc from the Galactic center, compared to only 20% for the LBA and EF samples, and to 3% for the subhalo population as a whole. The largest subhalos today are found at significantly larger radii than both the LBA and the EF subpopulation. A similar discrepancy has been previously pointed out by Kravtsov et al. (2004) and Willman et al. (2004), and may only partially be resolved by incompleteness in the census of distant Milky Way dwarfs or by numerical overmerging of subhalos in the inner 50 kpc of Via Lactea. Note that the luminous satellites appear to be biased towards the center even compared to the overall Via Lactea’s dark matter distribution.

The study of the central densities of dark-matter dominated dSphs offers another test of Λ CDM galaxy formation models and of the systematic small-scale properties – only minimally modified by baryonic effects – of their halos. To estimate the central mass density,

ρ_0 , of pressure-supported low luminosity dwarfs, a “core fitting” or King’s analysis is usually performed (King 1966; Richstone & Tremaine 1986). Under the assumption of spherical symmetry, close to dynamical equilibrium, mass following light, and isotropic stellar velocity dispersion, one has

$$\rho_0 = \frac{166\eta\sigma^2}{r_c^2} \text{ M}_\odot \text{ pc}^{-3}, \quad (7)$$

where σ is the observed central velocity dispersion in km s^{-1} , r_c the King profile core radius in pc, and η is a numerical parameter very close to unity. In two-component isotropic models in which luminous matter is negligible compared to dark matter and in which the core radius of the dark matter is larger than that of the visible material, equation (7) can overestimate the true central density by up to a factor of 2.2 (Pryor & Kormendy 1990). We have evaluated the central densities of Milky Way’s spheroidals from equation (7) (setting $\eta = 1$) using data in the literature. For the ultra-faint new dwarfs, King core radii have been estimated from published Plummer (half-light) radii r_P using $r_c = 0.64 r_P$ (Simon & Geha 2007). The radii and velocity dispersions assumed for this calculation, as well as our derived central densities, are given in Table 1. Central densities range from $\lesssim 0.1 \text{ M}_\odot \text{ pc}^{-3}$ (e.g. Hercules, Sextans, Canes Venatici I) to $\sim 1 \text{ M}_\odot \text{ pc}^{-3}$ (Ursa Major I, Coma Berenices, Leo T) to $\sim 20 \text{ M}_\odot \text{ pc}^{-3}$ (Willman 1). For comparison, we have computed the mean dark matter densities within 300 pc (about 3 times our force resolution) from their center, ρ_{DM} , for all Via Lactea’s subhalos. These are plotted in the left panel of Figure 8 as a function of peak circular velocity for subhalos at distances $R < 50 \text{ kpc}$, $50 < R < 200 \text{ kpc}$, and $200 < R < r_{200}$. These central densities increase steeply with circular velocities. In the smaller systems a distance of 300 pc is comparable to the radius where the peak circular velocity is reached, i.e. we probe scales where halo profiles are nearly isothermal and indeed the small systems follow the $\rho_{\text{DM}}(< 300 \text{ pc}) \propto V_{\max}^2$ scaling expected for isothermal halos quite well. The relation flattens for larger subhalos since their scale radii are larger than 300 pc and our measurements now probe the inner regions, which are shallower than isothermal.

The right panel of Figure 8 shows a comparison between the dark matter densities of subhalos in the LBA and EF sample and the central densities of dSphs. Via Lactea is clearly starting to resolve the inner dense regions of Milky Way-like satellites. In particular, the central densities of dSphs with measured core radii in excess of 250 pc (i.e. comparable to the radii within which ρ_{DM} is measured) appear to be in good agreement with the values found in subhalos of comparable circular velocities. A few satellites with core radii smaller than 100 pc, like Ursa Major II, Coma Berenices, and Willman 1, have central densities in excess of $1 \text{ M}_\odot \text{ pc}^{-3}$. The predicted dark matter densities we obtain by extrapolating inward the steep inner profiles of subhalos are perfectly consistent with the observed values. The left panel of the same figure also demonstrates that the typical central densities at a given V_{\max} are systematically larger for inner subhalos. This is a consequence of the larger average tidal mass loss suffered by this subpopulation: tidal

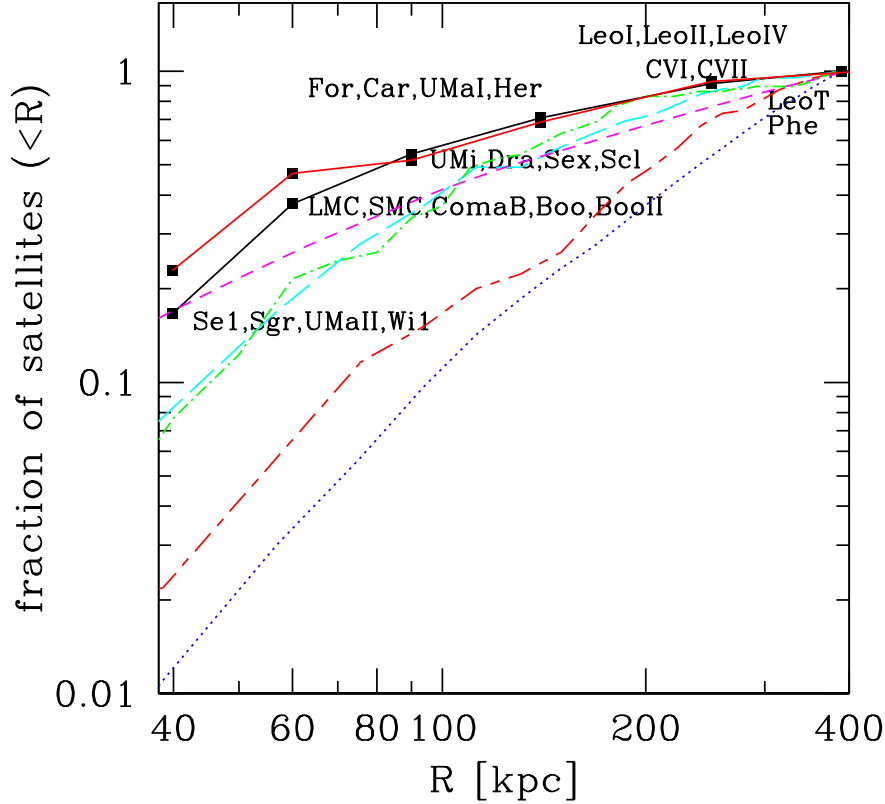


FIG. 7.— The normalized cumulative radial distribution of Milky Way satellites (*lower solid curve*). The upper solid curve connecting the squares shows the expected distribution of luminous satellites after correcting for the sky coverage of the SDSS. For plotting and comparison purposes, we have placed Leo T and Phoenix within $r_{200} = 389$ kpc. *Long-dashed curve*: distribution for the 65 largest $V_{\max,p}$ subhalos before accretion (Via Lactea LBA sample). *Dot-short dashed curve*: “fossil of reionization” EF sample. *Short-dashed-long dashed curve*: 65 largest V_{\max} Via Lactea subhalos today. *Dotted curve*: all 4021 Via Lactea subhalos with $M_{\text{sub}}/M_{\text{host}} > 10^{-6}$. *Short-dashed curve*: dark matter distribution.

stripping can significantly reduce V_{\max} without changing the central density, and inner subhalos end up having much larger typical concentrations (Diemand et al. 2007b). This concentration-radius relation should be taken into account when the central densities of luminous dwarfs (constrained by stellar kinematics) are used to infer the peak circular velocities of the host subhalos.

A simple way for estimating the range of host subhalo sizes corresponding to a given Milky Way satellite is to use the integrated dSph “central mass” within a physical radius comparable to the extent of the luminous region, and compare it to those of Via Lactea’s subhalos at similar galactocentric distances. The central masses $M_{0.6}$ (mass within 0.6 kpc) and $M_{0.1}$ (mass within 0.1 kpc) are robustly constrained by kinematic data. Given Via Lactea’s force resolution of 90 pc, $M_{0.6}$ is also robustly determined in simulated subhalos. $M_{0.1}$, however, is likely affected by gravitational softening and may be systematically underestimated. Here we use the most likely values and 90% confidence regions of $M_{0.1}$ from Strigari et al. (2007b) and of $M_{0.6}$ from Strigari et al. (2007a), as well as the best-fit $M_{0.6}$ values from Walker et al. (2007). We then find all Via Lactea

subhalos within 40% in distance and within 25% of the $M_{0.1}$ or $M_{0.6}$ values of each satellite, and then average over their V_{\max} and $V_{\max,p}$ to find the most likely host size.⁶ The range of plausible peak circular velocities was determined using all subhalos within the 90% confidence region in $M_{0.1}$ (or $M_{0.6}$). The results of this exercise are given in Table 2. Consistent with the expectations from the concentration-radius relation, for a given dSph central mass the most likely V_{\max} values of its host subhalos are larger at large galactocentric distances. If, e.g. Ursa Minor with $M_{0.6} = 5.3 M_{\odot}$ were to lie at a distance of 300 kpc, its most likely host would have $V_{\max,p} = 31 \text{ km s}^{-1}$ and $V_{\max} = 26 \text{ km s}^{-1}$. Coma Berenices with $M_{0.1} = 1.9 M_{\odot}$ at 300 kpc would typically be hosted by a $V_{\max,p} = 30 \text{ km s}^{-1}$ and $V_{\max} = 21 \text{ km s}^{-1}$ subhalo.

7. SUMMARY AND CONCLUSIONS

In this paper we have reported results from the two highest resolution simulations of Galactic CDM substruc-

⁶ For the dSphs marked with an asterisk in Table 2 no subhalos were found in the quoted range, and an estimate of the most likely host size was made using the subhalo with the smallest quadratic sum of the relative difference in distance and central mass.

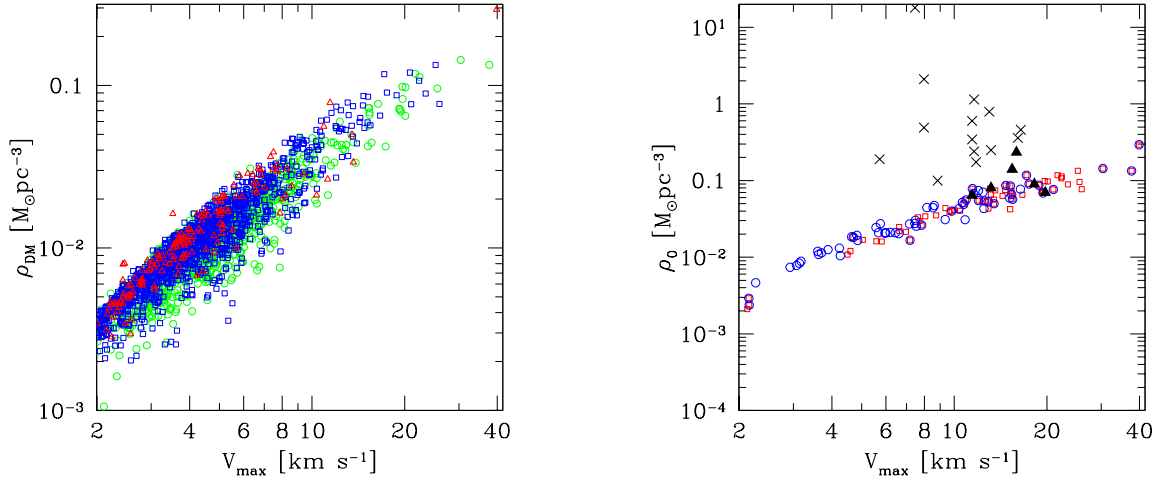


FIG. 8.— *Left panel:* Central dark matter densities (measured within the inner 300 pc) of Via Lactea subhalos as a function of their peak circular velocity today. *Triangles:* all subhalos within 50 kpc from the center. *Squares:* all subhalos between 50 and 200 kpc. *Circles:* all subhalos between 200 kpc and r_{200} . *Right panel:* Derived central densities of Milky Way dSphs, $\rho_0 = 166\sigma^2/r_c^2$, where σ is the stellar velocity dispersion in km s^{-1} and r_c is the King profile core radius in pc (see text for details). *Diagonal crosses:* dSphs with $r_c < 250$ pc. *Filled triangles:* dSphs with $r_c > 250$ pc. *Empty circles:* EF subhalo sample. *Empty squares:* LBA subhalo sample.

TABLE 2
LIKELY HOST SUBHALOS OF MILKY WAY SATELLITES

Name	Distance kpc	σ km s^{-1}	Central mass ^a $10^7 M_\odot$	$V_{\text{max,p}}$ km s^{-1}	V_{max} km s^{-1}	References
Ursa Major II*	38	6.7	$0.31^{+0.56}_{-0.1}$	50[15-67]	11[11-21]	(3)
Willman 1	43	4.3	$0.13^{+0.15}_{-0.08}$	37 [9-50]	14 [5-17]	(3)
Coma B	45	4.6	$0.19^{+0.21}_{-0.1}$	41 [14-63]	16 [8-18]	(3)
Ursa Minor	66	9.3	$0.23^{+0.19}_{-0.12}$	28 [14-63]	17 [8-21]	(3)
Sagittarius*	16	11.4	27^{+20}_{-27}	94	40	(1)
Ursa Minor	66	9.3	$5.3^{+1.3}_{-1.3}$	49 [35-63]	20 [17-22]	(1)
Draco	79	9.5	$4.9^{+1.4}_{-1.3}$	51 [30-67]	21 [21-23]	(1)
Draco*	79	9.5	6.9	35	22	(2)
Sextans	82	6.6	$0.9^{+0.4}_{-0.3}$	14 [8-23]	7 [6-9]	(1)
Sextans	82	6.6	2.5	25	14	(2)
Sculptor	86	6.6	$2.7^{+0.4}_{-0.4}$	26 [21-29]	15 [12-17]	(1)
Sculptor	86	6.6	4.3	32	23	(2)
Carina	101	6.8	$3.4^{+0.7}_{-1.0}$	29 [28-30]	18 [14-23]	(1)
Carina	101	6.8	2.0	25	12	(2)
Fornax	138	10.5	$4.3^{+2.7}_{-1.1}$	42 [21-63]	23 [15-26]	(1)
Leo II	205	6.6	$2.1^{+1.6}_{-1.1}$	21 [9-33]	13 [8-18]	(1)
Leo I	250	8.8	$4.3^{+1.6}_{-1.6}$	29 [21-35]	23 [15-26]	(1)

REFERENCES. — (1) Strigari et al. (2007a); (2) Walker et al. (2007); (3) Strigari et al. (2007b).

^a Equal to $M_{0.1}$ in the top 4 systems and to $M_{0.6}$ in all others. The quoted ranges are 90% confidence level regions.

* For these dSphs no subhalos were found in the quoted range, and an estimate of the most likely host size was made as described in the text.

ture to date, Via Lactea and 1e8Ell. The two runs follow the hierarchical assembly of a Milky Way-sized halo down to $z = 0$ and of an elliptical-sized halo down to $z = 0.5$, respectively, using different cosmological parameters. Our main findings can be summarized as follows:

1. Via Lactea and 1e8Ell are characterized by similarly steeply rising subhalo mass functions. In the range $200m_p < M_{\text{sub}} < 0.01M_{\text{host}}$, the best-fit slope of the differential distribution, $dN/dM_{\text{sub}} \propto M_{\text{sub}}^\alpha$, is $\alpha = -1.86 \pm 0.02$ for 1e8Ell and $\alpha = -1.90 \pm 0.02$ for Via Lactea. In the same mass range the cumulative mass function has slope -0.92 for 1e8Ell and -0.97 for Via Lactea. Compared to Via Lactea, 1e8Ell produces nearly a factor of two more subhalos with large circular velocities. When normalized to the maximum circular velocity of the host, the substructure circular velocity distribution yields 170 subhalos above $V_{\text{max}} = 22.5 \text{ km s}^{-1} = 0.056 V_{\text{host}}$ in 1e8Ell, compared to 110 above $V_{\text{max}} = 10 \text{ km s}^{-1} = 0.056 V_{\text{host}}$ in Via Lactea;
2. the fraction of the Via Lactea's host halo mass brought in by subhalos that have a surviving bound remnant today within r_{200} and with peak circular velocity $V_{\text{max}} > 2 \text{ km s}^{-1}$ is 45%. The total mass accreted in identifiable subunits exceeds 97%, as many major mergers at early times left no surviving $z = 0$ subhalos. Hence at our high resolution most of the Via Lactea mass is acquired in discrete clumps, with no significant contribution from smooth accretion. There are (14, 109, 873) subhalos today with $V_{\text{max}} > (20, 10, 5) \text{ km s}^{-1}$, which contributed (19, 30, 39)% of the mass of Via Lactea. Only 9-10% of the total material they brought in remains in self-bound surviving lumps at the present-epoch, the rest having been removed by tidal effects to become part of the “smooth” halo component. Mass losses are more severe for larger subunits.
3. because of tidal mass loss, the number of Via Lactea subhalos that have a surviving bound remnant today and reached a peak circular velocity of $> 10 \text{ km s}^{-1}$ throughout their lifetime exceeds half a thousand, five times larger than their present-day abundance and more than twenty times larger than the current (incomplete) tally of observed dwarf satellites of the Milky. The 20 largest V_{max} subhalos today have lost between 30% and 99.5% of the maximum mass that had before accretion. If substructure mass regulates star formation, then for a given mass threshold many more subhalos should have been able to build a sizeable stellar mass at some point in the past than indicated by their present-day abundance.
4. unless the circular velocity profiles of Galactic satellites peak at values significantly higher than

expected from the stellar line-of-sight velocity dispersion, only one out of five subhalos with $V_{\text{max}} > 20 \text{ km s}^{-1}$ today must be housing a luminous Milky Way dwarf. Any mechanism that suppresses star formation in small halos must start acting early, at redshift $z > 3$. Nearly 600 halos with masses greater than $10^7 M_\odot$ are found today in the “field” between r_{200} and $1.5r_{200}$, i.e. small dark matter clumps appear to be relatively inefficient at forming stars even well beyond the virial radius. Even if most subhalos appear to have no optically luminous counterparts, such a large substructure population may be detectable via flux ratio anomalies in strong gravitational lenses (e.g. Metcalf & Madau 2001), through its effects on stellar streams (e.g. Ibata et al. 2002; Mayer et al. 2002), or possibly via γ -rays from dark matter annihilation in their cores (Bergstrom et al. 1999; Stoehr et al. 2003);

5. the observed Milky Way satellites approximately follow the overall dark matter distribution of Via Lactea. They appear to be more biased to lie at small radii than both the LBA and the EF samples. The median distance of the observed satellites is 90 kpc, and the satellite distribution becomes even more compact after correcting for the SDSS sky coverage. This must be compared to a median distance of 110 kpc for the LBA and EF samples, and to 235 kpc for all Via Lactea subhalos. About 40% (50% after SDSS correction) of all Milky Way dwarfs are found within 60 kpc from the Galactic center, compared to only 20% for the LBA and EF samples, and to 3% for the subhalo population as a whole. Such discrepancies may only be partially resolved by incompleteness in the census of distant Milky Way dwarfs or by numerical overmerging in the inner 50 kpc of Via Lactea.
6. the study of the central densities of dark-matter dominated dSphs offers another test of Λ CDM galaxy formation models and of the systematic small-scale properties – only minimally modified by baryonic effects – of their halos. Via Lactea subhalos have central matter densities that increase with V_{max} and reach $\rho_{\text{DM}} = 0.1 - 0.3 M_\odot \text{ pc}^{-3}$, comparable to the central densities inferred in Milky Way dwarfs with core radii $> 250 \text{ pc}$.

P.M. acknowledges support from NASA grant NNG04GK85G. J. D. acknowledges financial support from NASA through Hubble Fellowship grant HST-HF-01194.01 awarded by the Space Telescope Science Institute, which is operated by the Association of Universities for Research in Astronomy, Inc., for NASA, under contract NAS 5-26555. M.K. gratefully acknowledges support from the Institute for Advanced Study. All computations were performed on NASA's Project Columbia supercomputer system.

REFERENCES

- Bellazzini, M., Gennari, N., & Ferraro, F. R. 2005, *MNRAS*, 360, 185
- Bellazzini, M., Gennari, N., Ferraro, F. R., & Sollima, A. 2004, *MNRAS*, 354, 708

- Belokurov, V., et al. 2006, *ApJ*, 647, L111
- Belokurov, V., et al. 2007, *ApJ*, 654, 897
- Benson, A. J., Lacey, C. G., Baugh, C. M., Cole, S., & Frenk, C. S. 2002, *MNRAS*, 333, 156
- Bergstrom, L., Edsjo, J., Gondolo, P., & Ullio, P. 1999, *PhRvD*, 59, 043506
- Bertschinger, E. 2001, *ApJSS*, 137, 1
- Bullock, J. S., Kravtsov, A. V., & Weinberg, D. H. 2000, *ApJ*, 539, 517
- Bullock, J. S., et al. 2001, *MNRAS*, 321, 559
- Coleman, M. G., Jordi, K., Rix, H.-W., Grebel, E. K., & Koch, A. 2007, *AJ*, 134, 1938
- Colín, P., Avila-Reese, V., & Valenzuela, O. 2000, *ApJ*, 542, 622
- Dekel, A., & Silk, J. 1986, *ApJ*, 303, 39
- Diemand, J., Kuhlen, M., & Madau, P. 2006, *ApJ*, 649, 1
- Diemand, J., Kuhlen, M., & Madau, P. 2007a, *ApJ*, 657, 262
- Diemand, J., Kuhlen, M., & Madau, P. 2007b, *ApJ*, 667, 859
- Diemand, J., Moore, B., & Stadel, J. 2004, *MNRAS*, 352, 535
- Dijkstra, M., Haiman, Z., Rees, M. J., & Weinberg, D. H. 2004, *ApJ*, 601, 666
- Dolphin, A. E., Weisz, D. R., Skillman, E. D., & Holtzman, J. A. 2005, in *Resolved Stellar Populations*, eds. D. Valls-Gabaud & M. Chavez (San Francisco: ASP), in press (astro-ph/0506430)
- Efstathiou, G. 1992, *MNRAS*, 256, 43P
- Gao, L., White, S. D. M., Jenkins, A., Stoehr, F., & Springel, V. 2004, *MNRAS*, 355, 819
- Grebel, E. K. 2000, in *Star Formation From the Small to the Large Scale*, eds. F. Favata, A. A. Kaas, & A. Wilson (Noordwijk: ESA), 87
- Harris, J., & Zaritsky, D. 2006, *AJ*, 131, 2514
- Hayashi, E., Navarro, J. F., Taylor, J. E., Stadel, J., & Quinn, T. 2003, *ApJ*, 584, 541
- Ibata, R. A., Lewis, G. F., Irwin, M. J., & Quinn, T. 2002, *MNRAS*, 332, 915
- Irwin, M. J., et al. 2007, *ApJ*, 656, L13
- Kamionkowski, M., & Liddle, A. R. 2000, *PhRvL*, 84, 4525
- Kazantzidis, S., Mayer, L., Mastropietro, C., Diemand, J., Stadel, J., & Moore, B. 2004, *ApJ*, 608, 663
- King, I. R. 1966, *AJ*, 71, 64
- Klypin, A. A., Kravtsov, A. V., Valenzuela, O., & Prada, F. 1999, *ApJ*, 522, 82
- Klypin, A., Zhao, H., & Somerville, R. S. 2002, *ApJ*, 573, 597
- Koposov, S., et al. 2007, *ApJ*, submitted (astro-ph/0706.2687)
- Kravtsov, A. V., Gnedin, O. Y., & Klypin, A. A. 2004, *ApJ*, 609, 482
- Kuhlen, M., Diemand, J., & Madau, P. 2007, *ApJ*, 671, 1135
- Kuhlen, M., & Madau, P. 2005, *MNRAS*, 363, 1069
- Machacek, M. M., Bryan, G. L., Abel, T., 2001, *MNRAS*, 320, 509
- Mac Low, M.-M., & Ferrara, A. 1999, *ApJ*, 513, 142
- Martin, N. F., Ibata, R. A., Chapman, S. C., Irwin, M., & Lewis, G. F. 2007, *MNRAS*, 380, 281
- Mateo, M. L. 1998, *ARA&A*, 36, 435
- Mateo, M., Olszewski, E. W., & Walker, M. G. 2007, *ApJ*, in press (astro-ph/0708.1327)
- Mayer, L., Kazantzidis, S., Mastropietro, C., & Wadsley, J. 2007, *Nature*, 445, 738
- Mayer, L., Mastropietro, C., Wadsley, J., Stadel, J., & Moore, B. 2006, *MNRAS*, 369, 1021
- Mayer, L., Moore, B., Quinn, T., Governato, F., & Stadel, J. 2002, *MNRAS*, 336, 199
- Metcalfe, R. B., & Madau, P. 2001, *ApJ*, 563, 9
- Moore, B., Diemand, J., Madau, P., Zemp, M., & Stadel, J. 2006, *MNRAS*, 368, 563
- Moore, B., Ghigna, S., Governato, F., Lake, G., Quinn, T., Stadel, J., & Tozzi, P. 1999, *ApJ*, 524, L19
- Moore, B., Quinn, T., Governato, F., Stadel, J., & Lake, G. 1999, *MNRAS*, 310, 1147
- Moore, B., Katz, N., & Lake, G. 1996, *ApJ*, 457, 455
- Mori, M., Ferrara, A., & Madau, P. 2002, *ApJ*, 571, 40
- Munoz, R. R., Carlin, J. L., Frinchaboy, P. M., Nidever, D. L., Majewski, S. R., & Patterson, R. J. 2006, *ApJ*, 650, L51
- Navarro, J. F., Frenk, C. S., & White, S. D. M. 1997, *ApJ*, 490, 493
- Navarro, J. F., & Steinmetz, M. 1997, *ApJ*, 478, 13
- Peñarrubia, J., McConnachie, A. W., & Navarro, J. F. 2007, *ApJ*, 672, 904
- Pryor, C., & Kormendy, J. 1990, *AJ*, 100, 127
- Reed, D., Governato, F., Quinn, T., Gardner, J., Stadel, J., & Lake, G. 2005, *MNRAS*, 359, 1537
- Richstone, D. O., & Tremaine, S. 1986, *AJ*, 92, 72
- Ricotti, M., & Gnedin, N. Y. 2005, *ApJ*, 629, 259
- Ryan-Weber, E. V., Begum, A., Osterloo, T., Pal, S., Irwin, M. J., Belokurov, V., Evans, N. W., & Zucker, D. B. 2007, *MNRAS*, in press (astro-ph/0711.2979)
- Simon, J. D., & Geha, M. 2007, *ApJ*, 670, 313
- Somerville, R. S. 2002, *ApJ*, 572, L23
- Spergel, D. N., et al. 2003, *ApJS*, 148, 175
- Spergel, D. N., et al. 2007, *ApJS*, 170, 377
- Stadel, J. 2001, PhD thesis, U. Washington
- Stoehr, F., White, S. D. M., Tormen, G., & Springel, V. 2002, *MNRAS*, 335, L84
- Stoehr, F., White, S. D. M., Springel, V., Tormen, G., & Yoshida, N. 2003, *MNRAS*, 345, 1313
- Strigari, L. E., Bullock, J. S., Kaplinghat, M., Diemand, J., Kuhlen, M., & Madau, P. 2007, *ApJ*, 669, 676
- Strigari, L. E., Koushiappas, S. M., Bullock, J. S., Kaplinghat, M., Simon, J. D., Geha, M., & Willman, B. 2007, *ApJ*, submitted (astro-ph/0709.1510)
- Thoul, A. A., & Weinberg, D. H. 1996, *ApJ*, 465, 608
- van den Bosch, F. C., Tormen, G., & Giocoli, C. 2005, *MNRAS*, 359, 1029
- van der Marel, R. P., Alves, D. R., Hardy, E., & Suntzeff, N. B. 2002, *AJ*, 124, 2639
- Walker, M. G., Mateo, M., Olszewski, E. W., Gnedin, O. Y., Wang, X., Sen, B., & Woodroffe, M. 2007, *ApJ*, 667, L53
- Walsh, S. M., Jerjen, H., & Willman, B. 2007, *ApJ*, 662, L83
- Weinmann, S. M., Macció, A. V., Iliev, I. T., Mellema, G., & Moore, B. 2007, *MNRAS*, 381, 367
- Willman, B., Governato, F., Dalcanton, J. J., Reed, D., & Quinn, T. 2004, *MNRAS*, 353, 639
- Willman, B., Masjedi, M., Hogg, D. W., Dalcanton, J. J., Martinez-Delgado, D., Blanton, M., West, A. A., Dotter, A., & Chaboyer, B. 2006, *AJ*, submitted (astro-ph/0603486)
- Yoshida, N., Abel, T., Hernquist, L., & Sugiyama, N. 2003, *ApJ*, 592, 645
- Young, L. M., Skillman, E. D., Weisz, D. R., & Dolphin, A. E. 2007, *ApJ*, 659, 331
- Zentner, A. R., Berlind, A. A., Bullock, J. S., Kravtsov, A. V., & Wechsler, R. H. 2005, *ApJ*, 624, 505
- Zentner, A. R., & Bullock, J. S. 2003, *ApJ*, 598, 49
- Zucker, D. B., et al. 2006, *ApJ*, 650, L41